Article

A Readout Scheme Providing High Spatial Resolution for Distributed Fluorescent Sensors on Optical Fibers

Barry J. Prince, Alan W. Schwabacher, and Peter Geissinger

Anal. Chem., **2001**, 73 (5), 1007-1015 • DOI: 10.1021/ac0011437

Anal. Chem. **2001,** *73,* 1007−1015

A Readout Scheme Providing High Spatial Resolution for Distributed Fluorescent Sensors on Optical Fibers

Barry J. Prince, Alan W. Schwabacher, and Peter Geissinger*

Department of Chemistry, University of Wisconsin—Milwaukee, P.O. Box 413, Milwaukee, Wisconsin 53201-0413

Optical fiber sensors using fluorescent probes distributed along the fiber cladding are of great interest for monitoring physical and chemical properties in their environment. The location of an emitting fluorophore along a fiber can be determined by measuring the time delay between a short, exciting laser pulse propagating in the fiber core and the returning fluorescence pulse. However, fluorescence lifetimes limit the spatial resolution, since a minimum separation of the fluorophores is required to resolve returning light pulses. For many applications, a closer spacing of sensor regions is desirable. We present a new method for the readout of closely packed fluorescent chemosensors located in the cladding of an optical fiber. By using a second fiber as an optical delay line, the minimum spacing between adjacent sensor regions can be well below the fluorescence lifetime limit. Since the coupling between the two fibers is evanescent, the attenuation of the excitation pulse is low, making long arrays of sensor regions feasible. This is particularly important since the one-dimensional combinatorial chemistry method developed by us allows for efficient preparation of diverse linear arrays. Detection sensitivities of 10^{-7} mol/L are demonstrated, with the potential for significant improvement.

In recent years, fiber-optic chemosensors have found increasing use for monitoring environmental conditions (pH, temperature, pressure, radiation, etc.) or for detecting the presence of substances in chemical or biological analytes (pollutants, toxins, antibodies, etc.). A typical configuration is to place the active sensor region on one end of the fiber, which allows efficient coupling of light from the fiber into the sensor and back into the fiber. Alternatively, the sensing region can be a continuous section of a fiber (distributed sensing) or a number of discrete regions along a fiber (quasi-distributed sensing). In both cases, the response of the sensor to a "triggering event" (e.g., a pressure change or the binding of a molecule) consists of changes in the light transmission or the light scattering of the fiber (for a review, see for example ref 1). Using a continuous light source, the signals detected at the end of the fiber are the cumulative response of all sensors to events occurring along the fiber.

Another rapidly growing chemosensor application is the microarray.[2] These arrays offer highly specific responses and discrimination between related analytes. A critical design issue is the independent addressing of each sensor region of the microarray. We demonstrate here that sensor regions distributed along an optical fiber have significant potential as chemosensor arrays of high spatial resolution, with excitation and readout carried out at the fiber termini. In optical fiber sensor arrays, the spatial location of sensors responding to triggering events can be determined using a method called optical time-domain reflectometry (OTDR). First used to locate faults in optical fibers,[3,4] it has now come into use for distributed fiber-optic sensors.[1,5,6] The basic scheme is the following: a laser pulse is coupled into the fiber, and upon encountering a sensor region, light scattered back is detected at the same end of the fiber with a characteristic time delay. This time delay encodes the spatial location of the scattering source along the fiber. A triggering event that changes the backscattered intensity is therefore easily located.

The use of fluorescent species as sensor molecules has the potential to provide much larger signals, since the quantum efficiencies for fluorescence may be orders of magnitude higher than those for scattering.[1,7,8] Placing fluorophores into the fiber core permits efficient collection of the emitted fluorescence. At the same time, however, this fluorescence doping increases the attenuation of the exciting light in the fiber. While for short fibers the increase in signal strength more than compensates for the higher losses in the exciting light,[9] these losses limit the overall length of the fiber sensor and, thus, the number of distinct sensor regions that can be placed on the fiber.

Placing the fluorescent sensor molecules into the cladding of the fiber can alleviate this problem. In practice, the existing cladding of the fiber is often replaced with a cladding that is (1) a suitable host material for the fluorescent sensors, (2) allows for the diffusion of the analyte to the sensor molecules, and (3)

* Corresponding author: (fax) (414) 229-5530; (e-mail) geissing@uwm.edu.

(1) Dakin, J. P. *Proc. SPIE−Int. Soc. Opt. Eng.* **1992**, *1797*, 76−108.
(2) Albert, K. J.; Lewis, N. S.; Schauer, C. L.; Sotzing, G. A.; Stitzel, S. E.; Vaid, T. P.; Walt, D. R. *Chem. Rev.* **2000**, *100*, 2595−2626.
(3) Ueno, Y.; Shimizu, M. *IEEE J. Quantum Electron.* **1975**, *QE-11*, 77D−78D.
(4) Ueno, Y.; Shimizu, M. *Appl. Opt.* **1976**, *15*, 1385−1388.
(5) Kvasnik, F.; McGrath, A. D. *Proc. SPIE−Int. Soc. Opt. Eng.* **1989**, *1172*, 75−82.
(6) Browne, C. A.; Tarrant, D. H.; Olteanu, M. S.; Mullens, J. W.; Chronister, E. L. *Anal. Chem.* **1996**, *68*, 2289−2295.
(7) Dakin, J. P. The Plessey Co., U.K. Patent GB 2156513A, March 28, 1984.
(8) Dakin, J. P. *J. Phys. E* **1987**, *20*, 954−967.
(9) Dakin, J. P.; Pratt, D. J. IEE Colloqium on Distributed Optical Fibre Sensors 74, London, 1986; p 10/1−6.

10.1021/ac0011437 CCC: $20.00
Published on Web 01/19/2001

preserves the guiding condition of the fiber. The latter condition implies that there is no refractive coupling of light from the fiber core to the cladding, meaning that fluorophores in the cladding can only be excited through the evanescent field of the core modes. Since evanescent coupling is weak, the attenuation of the light in the core is significantly less than for refractive coupling, making long arrays of chemosensors feasible. Moreover, since the evanescent field intensity drops off exponentially with distance from the core/cladding interface, only fluorophores close to this interface can be excited. The emitted fluorescence may be coupled back evanescently into the fiber core, which allows it to propagate under guided conditions back along the fiber to the detector, placed at the start of the fiber. Triggering a sensor molecule can result in changes of fluorescence intensity, fluorescence wavelength, and/or fluorescence lifetime. Evanescent excitation of fluorophores located in the fiber cladding and subsequent evanescent capture of the fluorescence by core modes were first combined with the OTDR method by Kvasnik and McGrath[5] and Chronister et al.[6]

For both core and cladding doping, the spatial resolution of the (quasi-)distributed fiber sensor is limited roughly by the fluorescence lifetime of the fluorophore. Yet, for many applications, the sensing regions should be closely spaced, particularly if only small quantities of analyte are available. Improving the limited spatial resolution is all the more desirable now that it is possible to prepare optical fibers containing thousands of discrete sensor regions using the novel one-dimensional combinatorial chemistry method developed recently by Schwabacher et al.[10,11] This new technique, first applied using cotton threads as linear supports, combines two previously incompatible, but highly desirable properties: the possibility of full library analysis and fully parallel synthesis. The procedure requires wrapping the linear support around cylinders of different, yet commensurate diameter for each reaction step (for details, see ref 11). The position of a reaction product on the linear support can always be identified with its synthetic history. Also, the reactions take place on many sections of the linear support simultaneously with each reagent handled only once per step, making the synthesis fully parallel. Evaluation of the combinatorial library can be carried out by treatment of the thread library with fluorophores. Localization of fluorescence at a particular region along the thread indicates binding to the library member in that position. The fluorescence properties of each region are monitored sequentially by pulling the thread through a fluorometer, resulting in a time trace of fluorescence signals.

Clearly, optical fibers constitute ideal linear supports for this scheme. Moreover, using the OTDR method, the evaluation of the combinatorial library can be carried out rapidly through the fiber itself.[12] However, due to the limited spatial resolution imposed by the fluorescence lifetimes of the fluorophores, such a fiber, providing, for example, a 25-ns detection window for each of 1000 regions, would be ~2.6 km long!

In this paper, we demonstrate that the use of a second fiber, serving as an optical delay line, overcomes this problem. One fiber contains the sensor regions that can be spaced within fractions of a millimeter. The second fiber periodically contacts the sensor regions, either—depending on the preferred configuration—providing evanescent excitation of the fluorophores or collecting evanescently the emitted fluorescence. For this scheme to work, the separation of two adjacent contact points along the second fiber has to be sufficiently large to create the required temporal separation. That is, the second fiber causes a delay in either the excitation pulse or the emitted fluorescence with respect to adjacent sensor regions on the first fiber. With this scheme, even for large numbers of sensor regions, one of the fibers can be very compact, allowing easy handling. After exposure of the sensor regions to the analyte, this fiber can be clamped onto the second fiber for readout and analysis.

In the following, we report on initial experiments that test the effectiveness of the fiber-to-fiber evanescent coupling scheme using four different fiber setups, each containing up to 10 individually prepared sensor regions. Up to four different fluorescent dyes were used on a fiber to show that wavelength discrimination is possible. The discussion also explores the prospects of extending the two-fiber scheme to large numbers of sensors.

OPTICAL-FIBER READOUT SCHEME

Light can propagate under guided conditions in an optical fiber by total internal reflection within the fiber core. The refractive indices of fiber core n_{co} and fiber cladding n_{cl} determine the critical angle $\Theta_z = \arcsin\{n_{cl}/n_{co}\}$ as well as the numerical aperture NA (or equivalently the half-angle α_c of the acceptance cone) of the fiber according to

$$\mathrm{NA} = n_{air} \sin \alpha_c = (n_{co}^2 - n_{c1}^2)^{1/2} \quad (1)$$

The number of optical modes N that a step profile fiber can sustain is given by[13]

$$N \cong V^2/2 \quad (2)$$

V is termed the fiber parameter[14] or the normalized frequency parameter[15,16] and can be written as

$$V = (2\pi r/\lambda) n_{co} \sin \Theta_c \quad (3)$$

where r is the radius of the fiber core and λ is the wavelength of the light in free space. The angle Θ_c complements the critical angle Θ_z and is therefore given by $\Theta_c = \arccos\{n_{cl}/n_{co}\}$. Equation 2 is valid for $V \gg 1$.

(10) Schwabacher, A. W. WiSys Technology Foundation, U.S. Patent Pending 09,253, 153, February 19, 1999.
(11) Schwabacher, A. W.; Shen, Y.; Johnson, C. W. *J. Am. Chem. Soc.* **1999**, *121*, 8669−8670.
(12) Schwabacher, A. W.; Geissinger, P. WiSys Technology Foundation, U.S. Patent Pending 09,535, 300, March 24, 2000.
(13) Payne, F. P.; Hale, Z. M. *Int. J. Optoelect.* **1993**, *8*, 743−748.
(14) Snyder, A. W.; Love, J. D. *Optical Waveguide Theory*; Chapman and Hall: London, U.K., 1983.
(15) Marcuse, D. *J. Lightwave Technol.* **1988**, *6*, 1273−1279.
(16) DeGrandpre, M. D.; Burgess, L. W. *Anal. Chem.* **1988**, *60*, 2582−2586.

Even under guided conditions, the electric field amplitude of a light mode in the fiber core extends into the fiber cladding as[17]

$$E(z) = E_0 \exp(-z/d_p) \tag{4}$$

where E_0 is the amplitude at the core/cladding boundary and z is the distance outside of the core boundary. The penetration depths d_p of these evanescent fields vary for each core mode according to[17]

$$d_p = \frac{\lambda}{2\pi n_{co}(\sin^2\Theta - \sin^2\Theta_z)^{1/2}} \tag{5}$$

where λ is again the free-space wavelength and Θ is the incident angle, which, for guided propagation, is greater than the critical angle Θ_z. This expression shows that (1) modes closer to Θ_z, (2) longer wavelengths (λ/n_{co}), and (3) larger critical angles all lead to increasing penetration depth.

Even if light propagates loss-free in the fiber core, chromophores present in the cladding within the range of the evanescent field can be optically excited, leading to an overall power loss in the fiber. For a multimode fiber with homogeneously distributed absorbers characterized by a cladding absorption coefficient α along a length l of the fiber, the overall ratio of output and input powers P_{out}/P_{in} is approximately given by[13,18]

$$P_{out}/P_{in} \cong V/\alpha l \tag{6}$$

The interesting fact that for increasing V a smaller proportion of the total light admitted into the fiber is available for interaction with absorbers in the cladding was pointed out in ref 16.

Following evanescent excitation, light emitted by fluorophores in the fiber cladding can couple back into the fiber core and propagate under guided conditions; light sources in the fiber cladding can interact with the evanescent tails of the guided core modes, transferring power to them.[15,19] Modes with a larger penetration depth d_p are able to collect more light those with smaller values of d_p, and by the same token, fluorophores located closer to the core/cladding boundary couple light more efficiently into the core. Calculations show that the overall light collection efficiency of a fiber, from sources distributed homogeneously in the cladding, depends roughly linearly on V and on the length of the region.[15] However, as stated above, the various core modes interact very differently with the light sources in the cladding. This is exemplified by the fact that for light sources located directly at the core/cladding interface, the collection efficiency is proportional to V^2, since all modes have reasonably high intensities at the interface.[15]

As indicated in the introduction, spatial information regarding the location of an emitting fluorophore along the fiber can be obtained using the OTDR method[3,4,20−22] (for a review, see ref 1).

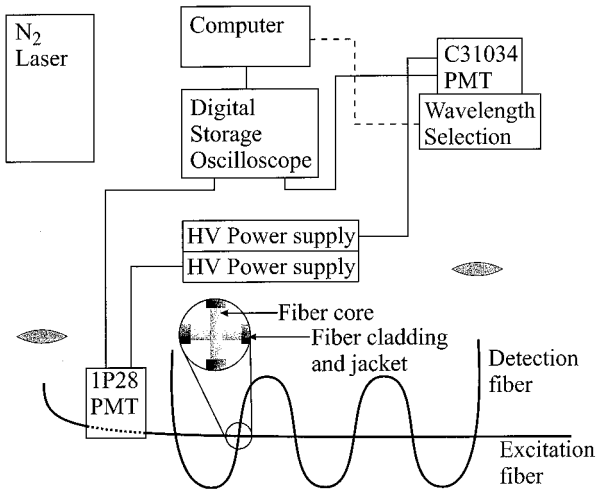

Figure 1. Basic experimental setup. The 1P28 PMT was positioned as shown for setup 1 only. Wavelength selection was performed with monochromators or color filters (see text). The enlargement shows a 90° fiber junction with claddings and jackets removed in the crossing region.

Laser pulses that are fed into the front end of the fiber cause pulsed evanescent excitation of the fluorophores.[6] The fluorescence "pulses" returning to the front of the fiber arrive with a time delay τ_d that allows for the calculation of the location L of the emitting fluorophore on the fiber according to

$$L = (c/2n_{co})\tau_d \tag{7}$$

Of course, many different sensor regions can be prepared along the fiber, allowing for the screening of a sample for many different substances. In this case, the data consist of a train of pulses, again encoding in the time domain the spatial location of the emitting molecules, revealing not only where an event takes place but also, if the sensor function in that region is highly selective, the identity of the substance causing the event. The spatial resolution, that is, the minimum separation of adjacent sensor regions, depends on the fluorescence lifetimes of the fluorophores. This is particularly critical if the sensor response to a triggering event is a change in the fluorescence lifetime of the fluorophore, in which case a detection time window of several times the fluorescence lifetime is needed for an accurate fit of the decay curves. According to eq 7, the required separation is $(0.15\ \text{m/ns})/n_{co}$, which yields, for a silica fiber with n_{co} =1.457 and a detection time window of 25 ns, a minimum separation of 2.57 m!

The readout scheme proposed here[12] employs two fibers: one fiber contains the sensor regions that are spaced much closer than the fluorescence lifetime limit, while the other fiber provides the optical delay needed to temporally separate the return signals (see Figure 1). Either fiber can be used for excitation or detection. If the fiber on which the sensor regions are prepared is used to carry the excitation pulse, the time delay between the excitation of adjacent sensor regions is negligible, but along the "detection fiber" the sensor regions are spaced much wider, so the return

(17) Harrick, N. J. *Internal Reflection Spectroscopy*; Interscience Publishers: New York, 1967.
(18) Egalon, C. O.; Mendoza, E. A.; Khalil, A. N.; Lieberman, R. A. *Opt. Eng.* **1995**, *34*, 3583−3586.
(19) Christensen, D.; Andrade, J.; Wang, J.; Ives, J.; Yoshida, D. *Proc. SPIE−Int. Soc. Opt. Eng.* **1989**, *1172*, 70−74.
(20) Barnoski, M. K.; Jensen, S. M. *Appl. Opt.* **1976**, *15*, 2112−2115.
(21) Barnoski, M. K.; Rourke, M. D.; Jensen, S. M.; Melville, R. T. *Appl. Opt.* **1977**, *16*, 2375−2379.
(22) Personick, S. D. *Bell Syst. Technol. J.* **1977**, *56*, 355−366.

signals are spaced in time accordingly. In this case, the location along the fiber is given by

$$L = (c/n_{co})\tau_d \quad (8)$$

The factor of $^1/_2$ appearing in eq 7 is absent here. In the case where the "excitation fiber" provides a time delay between the excitation of adjacent, closely spaced sensor regions on the detection fiber, eq 8 still holds true. In both cases, the location L refers to the fiber providing the optical delay.

For both the one- and two-fiber schemes, a time reference is needed. The front-end reflection of the input pulse provides this reference in the one-fiber scheme, while in the two-fiber scheme, a fluorescent reference can be prepared on the fiber at a known position for this purpose.

EXPERIMENTAL SECTION

The results described below were obtained using four different experimental setups. Figure 1 shows a schematic representation that illustrates the basic features of all four setups. Two fibers were used: the excitation fiber carried the 337-nm light pulses from a Photon Technology International PL2300 nitrogen laser (typically 0.6-ns pulse width and 1.4-mJ pulse energy with repetition rates of 3−10 Hz) to the sensor regions, and the detection fiber delivered the resulting fluorescence to a Burle C31034 (2.5-ns rise time) photomultiplier tube (PMT). Longer wavelength excitation could be achieved using a dye laser (Photon Technology International PL201) pumped by the nitrogen laser. The resulting signals were collected on either a Hewlett-Packard HP54505B or LeCroy LC564DL digital storage oscilloscope (DSO) with respective bandwidths of 300 MHz and 1 GHz and sampling rates of 500 MSa/s and 4 GSa/s, respectively. A trigger for the DSO was generated using a second PMT (RCA 1P28, 1.6-ns rise time), which collected light scattered from the front of the excitation fiber. For setup 1, the excitation fiber passed through the housing of the 1P28 PMT (as depicted in Figure 1). In this case, the PMT measured light escaping from the side of the fiber (largely cladding fluorescence, although there may have been contributions due to refractive losses of modes that were coupled into the fiber under nonguiding conditions, and scattered light from core inhomogeneities) and therefore provided a measure of the total intensity of light in the fiber, while still providing the trigger signal. The spectral decomposition of the signal, if used, was obtained using colored glass filters, a Jobin Yvon H10 monochromator (0.1-m focal length, 8 nm/mm linear dispersion), or a Jarrell Ash 82-000 monochromator (0.5-m focal length, 1.6 nm/mm linear dispersion).

The sensor regions themselves were prepared by removing the fiber jacket and cladding at the junction(s) of the two fibers so that the two fiber cores, at an angle of 90° to one another, were just touching. Therefore, the contact pressure was minimal, governed only by the weight of the top fiber. The junctions were then immersed in a solution of a fluorescent dye in a solvent with a refractive index that preserved the guiding condition of the fiber. In Figure 1, the detection fiber provides an optical delay between detection of the fluorescence from adjacent regions; however, in setup 4, the two fibers of Figure 1 are reversed so that there is a delay between *excitation* of adjacent regions. In the three setups that contain multiple fiber junctions, the separation between adjacent regions along the fiber providing the optical delay was typically 2 orders of magnitude greater than their separation with respect to the other fiber.

All setups used multimode silica fibers with a TECS (trademark of 3M Corp.) cladding (Thorlabs/3M FT-200-UMT and FT-400-UMT with core diameters of 200 and 400 μm, respectively). All fibers had core and cladding refractive indices of n_{co} =1.457 and n_{cl} =1.404, respectively. Although the TECS cladding shows some absorption in the UV region leading to transmission losses in the fiber, its use is advantageous since the cladding can be removed with acetone, thereby preserving the core surface. This avoids the HF treatment often applied for the removal of silicone claddings, which may etch the core surface and lead to refractive losses.

The first fiber setup was used for measuring the sensitivity of evanescent coupling between the two fibers: a 400-μm fiber for excitation and 200-μm fiber for detection. A single junction was located ∼1 m along the excitation fiber. The fluorescence signal traveled through 500 m of the detection fiber to the detector, which delayed the arrival time of the signal at the detector by ∼2.5 μs (until the rf emission accompanying the discharge of the nitrogen laser had subsided to a negligible level).

The second setup was used to test the attenuation of the exciting light pulse when multiple sensor regions are present on the fiber. For these experiments, a 200-μm fiber was coiled up on a 20-cm-diameter cylinder. Every nine windings (corresponding to a separation of 5.84 m or 28 ns), 1 cm of the fiber core was exposed. A 400-μm fiber with cladding and jacket removed touched each of these exposed regions. The crossing points were ∼1 cm apart along the 400-μm fiber. Six fiber−fiber coupling regions were created in this way and submerged in a 2×10^{-5}-mol/L aqueous solution of Rhodamine 590 (R6G). The refractive index of this solution (approximately that of water) ensured that the guiding conditions of both fibers were retained throughout the regions in which their claddings were removed.

While the first two setups were used to investigate the basic properties of the fiber−fiber coupling scheme, the third was prepared to test how a number of closely packed sensor regions containing different dyes (Stilbene 420 (S420), Coumarin 500 (C500), R6G, LDS698—all Exciton) can be spatially and spectrally resolved. Here, 10 regions were prepared, separated by only three windings (∼9.5 ns) of the detection fiber. The regions were then immersed in a drop of agarose gel swelled with water containing the dye molecules of interest. These sensor regions were spaced by ∼5 mm along the 400-μm-diameter excitation fiber. The dyes in each sensor region, from the end of the detection fiber closest to the detector, were as follows: S420; LDS698; R6G; C500; S420; LDS698; C500; S420; LDS698; C500.

For the fourth setup, six sensor regions (again immersed in agarose gel, the first three adjacent regions along the excitation fiber containing LDS698, the remaining three containing S420) were prepared. In this case, the excitation fiber was used as the optical delay line. Both the excitation and detection fiber had a core diameter of 400 μm. The sensor regions were separated by nine windings (∼29 ns) of the excitation fiber and ∼1 cm along the detection fiber.

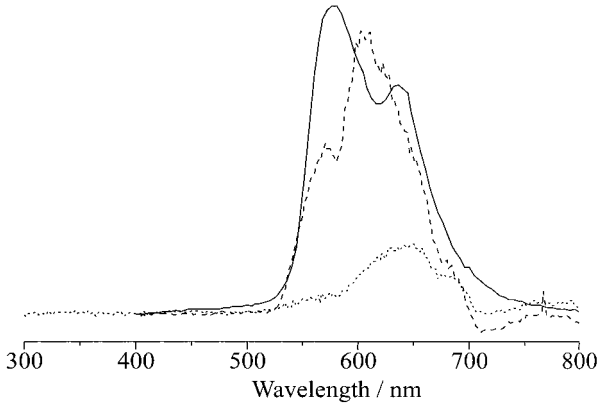

Figure 2. Spectra of signals (plotted on the same scale) detected after passing through 500 m of fiber with the sensor region submerged in water only (dotted line) and in a 10^{-4} M aqueous solution of R6G (dashed line). The solid line shows a fluorescence spectrum of an aqueous solution of R6G for comparison.

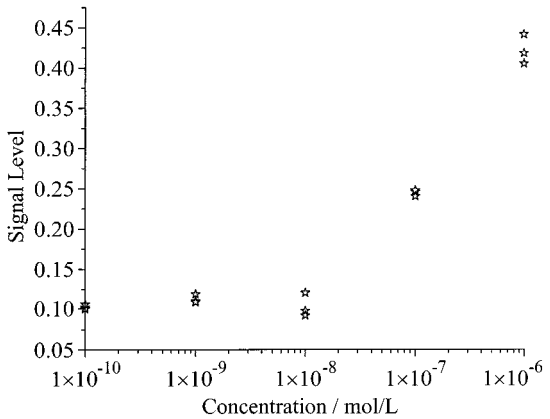

Figure 3. Signal intensity after passage through 500 m of fiber versus R6G concentration using setup 1. Data for three separate measurements are shown for each concentration.

RESULTS

Setup 1: Sensitivity of Coupling. Our initial experiments, using setup 1, focused on the efficiency of evanescent fluorophore excitation and subsequent evanescent coupling into a second fiber and on the sensitivity of such a measurement. The silica/TECS fiber that was used in these studies satisfied two important criteria: the silica core enabled the use of a UV excitation source, and the TECS cladding could be easily removed for simple preparation of fiber−fiber junctions. However, when coupling 337-nm light pulses into these fibers, strong luminescence is observed from the cladding. Presumably this is fluorescence from the TECS cladding itself, which may be excited evanescently by the laser pulse (there may also be some excitation of the TECS cladding due to light coupled into the fiber under nonguiding conditions, but the population of these modes is expected to be small). As well as significantly attenuating the laser pulse in the fiber, this luminescence can evanescently couple back into guiding modes of the fiber leading to a broad distribution of wavelengths within the fiber core.

To minimize the transmission of light from the excitation fiber directly into the detection fiber at the point of contact, the fibers were crossed at right angles at the fiber junctions (see inset in Figure 1). Figure 2 shows the spectrum obtained from setup 1 when the fiber junction was submerged in only water (dotted line) and in a 10^{-4} mol/L aqueous solution of R6G (dashed lines). These spectra were generated by focusing the light from the detection fiber into the 0.1-m monochromator. For each wavelength, 100 signal traces were averaged on the DSO and the total trace was integrated to obtain the averaged fluorescence intensity. It can be seen that there is leakage of light across the fibers even in the absence of fluorophores at the fiber junction. It is thought that this signal is due to cladding luminescence passing into the detection fiber along with the excitation pulse, which subsequently leads to additional cladding luminescence in the detection fiber. The maximum in this signal, which occurs at ∼640 nm, does not reflect the wavelength of maximum cladding luminescence, but rather the wavelength of minimum attenuation for this fiber (for a fiber attenuation spectrum, see ref 23; recall that in this experiment the light must pass through 500 m of the fiber before reaching the detector, which essentially removes any light at 337 nm that enters the detection fiber). This point is further illustrated by the red shift in the fluorescence of R6G when observed after passing through the 500-m fiber (Figure 2, solid line). Moreover, experiments using the dye laser revealed that excitation wavelengths above ∼420 nm do not cause cladding luminescence—in this case, a small amount of the exciting light still leaks into the detection fiber and is detected without change in wavelength.

To determine the sensitivity of the measurements in the evanescent fiber−fiber coupling scheme, the R6G concentration was increased by factors of 10 starting from a solution of 10^{-10} mol/L until an R6G fluorescence signal could be discerned above the level of the background signal. Since the background signal and R6G fluorescence overlapped, the monochromator was removed, and all light exiting the detection fiber was focused directly into the PMT in order to maximize the detection sensitivity. The average of 1000 time traces obtained for each concentration was integrated and divided by the integrated reference time trace. The results are depicted in Figure 3. An R6G concentration of 10^{-7} mol/L can be easily detected above the background signal.

Setup 2: Attenuation of Light in the Fiber. One of the goals of this work was to investigate whether the evanescent fiber−fiber coupling scheme is suitable for long arrays of fiber sensors. A primary concern is the attenuation of the exciting and signal pulses. To test the extent of attenuation in both the excitation and detection fibers, six regions were prepared in an aqueous solution of R6G (see the description of setup 2 above). The four traces shown in Figure 4 were each obtained by averaging 64 time traces. They were recorded from each end of the detection fiber (labeled D_1 and D_2) for excitation from both ends, E_1 and E_2, of the excitation fiber. Therefore, the labels E_i in Figure 4 indicate the fiber end that admits the laser pulses, while D_i specifies at which end of the detection fiber the fluorescence was collected. The sensor regions were numbered 1−6 from the E_1 (D_1) end of the fiber to the E_2 (D_2) end. In this setup, the detection fiber provided the optical delay for the fluorescence signals, so the D subscript specifies the order in which the fluorescence signals from each region arrived at the detector; for E_1D_1 and E_2D_1, the data pulses arrived in the order from 1 to 6, whereas for E_1D_2 and E_2D_2 the data pulse sequence is from 6 to 1.

(23) Thorlabs/3M, http://www.thorlabs.com/thorcat/Main/0258−000.HTML, 2000.

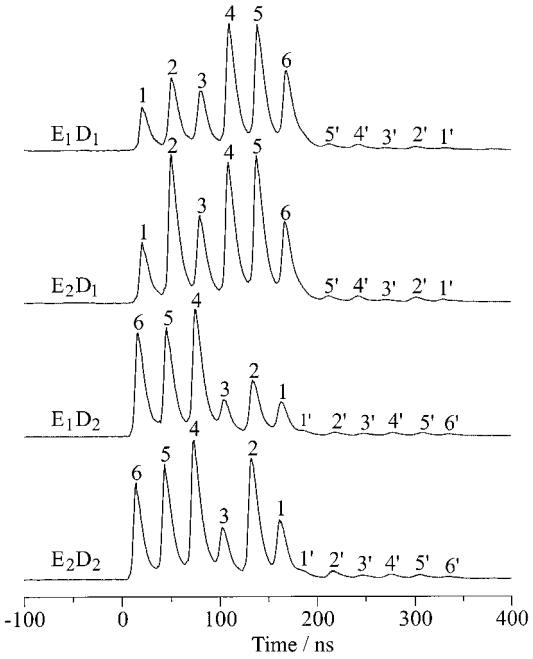

Figure 4. Signal traces obtained from setup 2 using six sensor regions. The labels are explained in the text. All traces are plotted on the same scale.

The overall intensity of the four traces collected was expected to vary due to slight differences in the efficiency of coupling light into or out of the ends of the fibers, but variations in the *relative* peak intensities of each trace provide information about the loses within the excitation and detection fibers. The differences in relative peak intensities between the E_1D_1 and E_2D_1 traces, and between the E_1D_2 and E_2D_2 traces, can be attributed to attenuation of the exciting light in the excitation fiber between regions 1 and 6; with zero attenuation in this fiber, these traces will be exact duplicates. Similarly, the difference in relative peak intensities between E_1D_1 and E_2D_1, and between E_1D_2 and E_2D_2, can be attributed to attenuation of fluorescence in the detection fiber between regions 1 and 6; with zero attenuation in this fiber, these traces will exactly mirror one another. Although there are slight variations in the relative peak intensities of the four traces in Figure 4, the overall pattern remains, suggesting that there is little attenuation of light in the excitation and detection fibers. This observation is corroborated by the presence of a second set of peaks, which are labeled 1′−6′ in Figure 4. These peaks arise from reflections of the sensor fluorescence from the far end (i.e., the nondetection end) of the fiber. In fact, for D_1 detection, the 6′ peak is unresolved from 6 since region 6 is too close to the end of the detection fiber. It is remarkable that, for example, in the D_2 traces, the 6′ peak, which travels the length of the fiber twice and passes by 11 sensor regions before reaching the detector, is of comparable intensity to the 1′ peak, which travels the length of the fiber only once and passes by 6 sensor regions, demonstrating again that the losses in the detection fiber are low. These observations are discussed in more detail in a subsequent paper.[24]

Setup 3: Multiple Dyes. Having demonstrated the feasibility of evanescent coupling between two fibers, we turn to fiber setup 3, in which four different dyes were distributed among 10 sensor regions. Figure 5a shows the cumulative signal for all wavelengths, obtained by focusing the emission from the detection fiber directly into the PMT without spectral decomposition and by averaging 16 traces. The individual regions are not resolved in this case, leading to only two broad bands being detected. (The band marked with the arrow in the figure again arises from reflections at the remote end of the detection fiber leading to light propagation back down this fiber to the PMT.) The reason for the limited temporal resolution is that the spacing of adjacent fiber regions along the detection fiber (which provides the optical delay in this case) is only ~9.5 ns—approximately equal to the fluorescence lifetimes of these dyes. Still, by employing wavelength-selective devices, the signals from the individual regions can be distinguished. Using the 0.5-m focal length monochromator for the spectral decomposition of the light exiting the detection fiber and averaging 128 of the resulting traces yields the surface plot shown in Figure 5b, in which the emission of the fiber is plotted versus

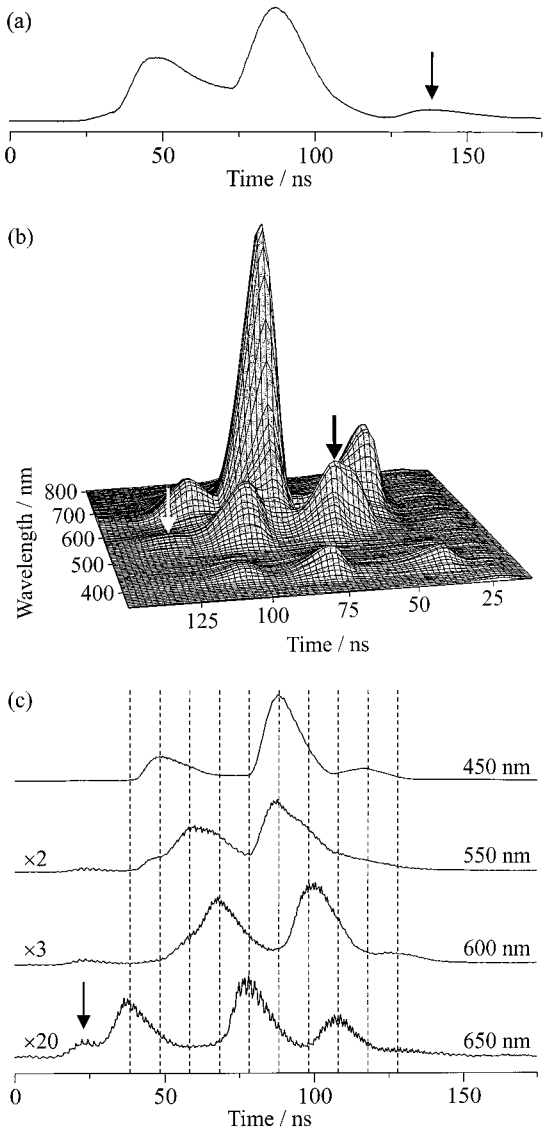

Figure 5. Signal obtained with setup 3 containing 10 sensor regions. (a) Integrated signal (all wavelengths) versus time. The black arrow marks the band caused by reflections at the far end of the detection fiber. (b) Signal strength plotted versus time and detection wavelength. The features marked by the arrows are referred to in the text. (c) Fixed wavelength sections taken from the surface shown in (b).

(24) Prince, B. J.; Schwabacher, A. W.; Geissinger, P., in preparation.

wavelength and time of detection. Although 8 peaks are clearly discernible in this figure, in fact, all 10 sensor regions are represented. The white arrow marks the very weak signal from region 10, and the black arrow indicates the still-unresolved signals from regions 4 and 5. More detailed information can be obtained by taking cross sections from the surface plot at fixed wavelengths. This is shown in Figure 5c for the wavelengths 450, 550, 600 and 650 nm. The equally spaced, vertical lines in the figure show the times at which detection of the signals from each of the 10 sensor regions was expected. While the coupling efficiency varies significantly for the different regions (presumably due to microscopic differences in the geometry of the fiber junctions), all 10 regions are accounted for. The S420 sensors at regions 1, 5, and 8 all appear in the 450-nm trace, the C500 regions, 4, 7, and 10, dominate the detected signal at 550 nm, and the LDS698 regions 2, 6, and 9 appear at 650 nm. The R6G sensor at region 3, although not completely resolved from the adjacent LDS698 or C500 regions, is clearly visible in the 600-nm section. The peak marked with an arrow in the 450-nm trace of Figure 5c is actually present, with equal intensity, in all traces and can also be seen as a weak, wavelength-independent ridge at 25 ns in Figure 5b. This signal is not due to fluorescence from a sensor region, but rather occurs due to weak laser reflections that do not pass through the fiber setup and monochromator, but are detected directly by the PMT.

These results show that even when the sensor regions are closely spaced along the fiber, which provides the optical delay, they may still be spectrally resolved. It should be noted that the fluorescent signal from one region could be reabsorbed by a different dye in a subsequent region (for example, the S420 from regions 5 and 8 passes two regions containing LDS698, 2 and 6, which can be excited in this way). The significance of reabsorption processes for the design of large fiber arrays requires further study.

Setup 4: Effects of Refractive Index Changes. Finally, using setup 4, we investigated the effect of refractive index changes of the sensor region on the fiber−fiber coupling. The agarose gel, when swelled with water, has a refractive index approximately equal to that of water, ensuring that the guiding condition of the fiber is maintained. As the gel dries, however, the refractive index gradually increases to a final value of ∼1.51—well in excess of the fiber core index—such that the coupling between the two fibers is refractive. The three traces shown in Figure 6, each generated by averaging 512 time traces from the fluorescence signal of the six agarose-clad regions, shows the effect of the drying gel. In the bottom trace, collected immediately after the agarose gel was prepared, only four of the six regions can be discerned. After letting the agarose regions dry for 2 h, fluorescence signals of all six regions can be detected. The overall intensity has increased significantly, and the relative intensity of the six regions has also changed. After drying for 26 h, the overall intensity of the signal increased significantly again and the relative intensities were again redistributed. A more detailed study of the effect of refractive index changes on coupling efficiency will be presented elsewhere.[24]

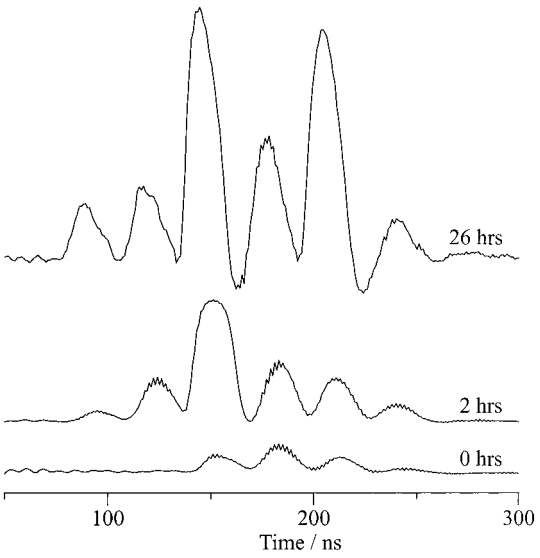

Figure 6. Changes of the signal intensities caused by refractive index changes, which result from the drying of the agarose cladding in six sensor regions. The traces are labeled with their respective drying times.

DISCUSSION

Our results clearly demonstrate that the two-fiber scheme can overcome the problem of limited spatial resolution found in fluorescent chemosensors on optical fibers. Although in these studies the sensor regions were separated by 5−10 mm, a further reduction is possible. A practical limit is given by the diameter of the fiber providing the optical delay; the penetration depth of the evanescent waves imposes a theoretical limit. As long as the fiber junctions are separated by ∼5λ, where λ is again the wavelength, the probability that the fluorescence from one sensor region is picked up at two regions on the detection fiber or that one sensor region is excited repeatedly from two regions on the excitation fiber is negligible.

Combining the temporal resolution afforded by the delaying fiber with a spectral decomposition of the signals, as shown in Figure 5, allows for a reduction of the spacing of the regions along the *delaying* fiber. In this case, the fluorescence signals of all 10 sensor regions were detected, albeit at different intensities due to different coupling strengths and fluorescence quantum yields. Moreover, spectral decomposition allows for the incorporation of multiple dyes into one sensor region, as long as the fluorescence bands of these dyes do not overlap and the interaction of these dyes does not lead to fluorescence quenching.

The sensitivity of the evanescent fiber−fiber coupling determined here is remarkable considering the fairly large background signal against which the fluorescent signals were detected. As shown in Figure 2, even for a 10^{-4} mol/L solution of R6G, the fluorescence detected is only ∼4 times that of the background signal, and yet the signal-to-noise ratio (S/N) is sufficient that the fluorescence from a solution 3 orders of magnitude more dilute can still be clearly detected above the background. By choosing a fiber with a silica cladding, more transparent to the UV excitation source, or by using a longer-wavelength light source for excitation, this background luminescence should be effectively eliminated, leading to a significant improvement in S/N and, therefore, an enhancement of the sensitivity.

It is also worthy of note that unlike the previous experiments of Kvasnik and McGrath[5] and Chronister et al.,[6] which utilized a single fiber for both excitation and detection, and probed sensor regions which spanned ∼25 and ∼4 cm (respectively) of the fiber, the sensor regions probed here are orders of magnitude smaller.

Assuming the sensor regions encompass only the volume, which lies within $\sim 5\lambda$ of the point of contact between the two fibers, which amounts to an effective sample volume of $\sim 10^{-12}$ L. The precise volume is defined by the penetration depths of the two fibers' modes. It is thus, all the more remarkable that this technique, in which such small volumes are probed, is as sensitive as we have determined here.

For the data collected using setup 1, all detectable contributions to the noise were stochastic in nature. Thus, although the points plotted in Figure 3 were the result of averaging 1000 traces, the LeCroy DSO has the capability of averaging 10^6 traces, providing the potential for a further 30-fold increase in S/N. At the present time, such an experiment is not feasible due to the slow repetition rate of the laser (recording 10^6 traces at 10 Hz would take $\sim$28 h). Employing an excitation source with higher pulse repetition rates will further enhance the sensitivity of this readout scheme.

The signals are increased further when the full numerical aperture of the fiber (eq 1) is used. Increasing the input cone angle of the light coupled into the fiber leads to an increasing population of modes closer to the critical angle. According to eq 5, these modes have larger penetration depths d_p and larger values of E_0, which leads to a higher probability of excitation. Moreover, increasing the input numerical aperture also increases the total number of modes in the fiber as[13,25]

$$N(\Theta_{in}) = \frac{V^2}{2} \frac{\Theta_{in}^{\ 2}}{\sin^2 \Theta_c} \tag{9}$$

where Θ_{in} is the half cone angle of the light pulse that is focused on the front end of the fiber. This expression is valid for weakly guiding fibers. The cumulative effect is higher levels of evanescent excitation in the cladding, leading to larger fluorescent signals.

As in any type of fluorescence experiment, the signal intensities depend on a number of geometrical parameters. In our case, the exact geometry at the fiber−fiber junction will be of great importance. Even for otherwise identical regions, a slight variation in the separation of the two fibers leads to an exponential variation in the resulting signal. This can be seen by superimposing the exponential decay of the evanescent tail (see eq 4) of the excitation fiber with the corresponding exponential increase for evanescent capture toward the detection fiber. Moreover, in multimode fibers, the intensity distribution of modes changes from one region to the next; since the losses are strongest for modes near the critical angle, these tend to be reduced in intensity first, which implies that signals from an array of otherwise identical sensors will exhibit declining signal intensities. Continuous scrambling of the modes, which can be achieved, for example, by imposing a high curvature on the fiber, can counteract this effect.

It has to be pointed out that, as in the one-fiber OTDR scheme, two evanescent coupling steps are involved: transfer of exciting light and capture of emitted light. In contrast to the one-fiber scheme, however, the two-fiber scheme offers more flexibility since fiber parameters (like core diameter, refractive indices, and numerical aperture) can be optimized separately for each of the excitation and detection fibers. This flexibility is particularly important for the long arrays of sensors envisioned here. The magnitude of the losses in the exciting fiber can be controlled to some extent by the choice of refractive indices (eqs 3 and 6). Likewise, the detection fiber can be optimized in this way for maximum capture efficiency. Furthermore, the value of E_0 in eq 4 and the penetration depth d_p (eq 5) depend on the fiber parameters and on the particular core mode.[17] According to eq 9, the range of core modes can be controlled to some extent by the cone angle of the light focused into the end of the fiber. The total amount of light that a fiber accepts increases with the number of guiding modes it can support (eq 2), which again is directly related to the basic fiber parameters.[25]

As mentioned in the introduction, the novel one-dimensional combinatorial chemistry method allows for the methodical building of long arrays of fiber sensors for many purposes. For the optical evaluation of these sensor arrays, issues of light attenuation in the fibers become crucial. For UV excitation pulses, the dominant loss mechanisms in the fiber core are Rayleigh scattering and impurity absorption (e.g., trace amounts of metal ions).[26] The fluorescence signals are also affected by Rayleigh scattering, although the ω^4 dependence ensures that this contribution diminishes for longer wavelengths. Above 700 nm, OH absorption starts to become the limiting factor for fiber clarity.[26−28] Absorption and scattering by the cladding may lead to additional losses. For the fibers and excitation wavelengths used in this work, the latter effect is likely to dominate the overall losses. The data presented in Figure 4 show that the overall attenuation is small. As Figure 2 shows, however, for long fibers, the fiber transmission characteristics modify the fluorescence band shapes of the fluorophores.

Moreover, in long fibers, intermodal and intramodal dispersion can lead to a broadening of the input and signal pulses affecting the temporal and thereby the spatial resolution. In multimode fibers, the intermodal dispersion due to the different paths that light can take in the fiber is usually dominant. According to ray optics, the temporal stretching per unit length $\Delta\tau_d$ of a δ-shaped input pulse is given by

$$\Delta\tau_d = \frac{1}{c} \frac{n_{co}}{n_{cl}} (n_{co} - n_{cl}) \tag{10}$$

This means that the spatial separation of adjacent sensor regions along the fiber has to increase accordingly. For the 500-m fiber used in setup 1, a δ-shaped input pulse would be stretched to $\sim$90 ns. First results show that this is not the case for the signal pulses, the reason being that the evanescent capture of the fluorescence is accomplished predominantly by a subset of modes close to the critical angle. Therefore, the signal dispersion is expected to be significantly less than predicted by eq 10. This important issue will be addressed in more detail in a subsequent paper.[24]

Last, we showed that a change of the refractive index of the substance replacing the cladding has a profound influence on the

(25) Gloge, D. *Appl. Opt.* **1971**, *10*, 2252−2258.

(26) Keck, D. B.; Maurer, R. D.; Schultz, P. C. *Appl. Phys. Lett.* **1973**, *22*, 307−309.

(27) MacChesney, J. B.; DiGiovanni, D. J. *J. Am. Ceram. Soc.* **1990**, *73*, 3537−3556.

(28) Thomas, G. A.; Shraiman, B. I.; Glodis, P. F.; Stephen, M. J. *Nature* **2000**, *404*, 262−264.

signals. Not only are the overall intensities affected but also the relative intensities of the signals of the individual regions. Clearly, the losses that occur at the sensor regions under refractive conditions will prohibit the creation of long arrays of sensors. It is interesting to note that as the refractive index of the sensor region increases, the peak intensities are not dramatically shifted in favor of the first excited regions, even though these received the most excitation intensity. However, in this setup, the fluorescence signal of the first region to be excited (containing LDS698) had to travel past the other regions to reach the detector. At each region the signal passed, it incurred strong refractive losses. Therefore, the fluorescence signal from the first region is attenuated most strongly. Consequently, the relative changes in peak intensities upon increasing the refractive index are difficult to predict. Since the S420 fluorescence reaches the detector without passing the LDS698 regions, reabsorption is unlikely to play a role here.

Further reduction of the spatial separation can also come from use of light scattering particles as sensors, due to the much shorter time scale. In general, fluorescence is preferable to light scattering, because of its intensity and wavelength shift; however, scattering caused by particles at the core surface can be very large in special cases.[29,30]

In summary, we have demonstrated that the spatial resolution for the readout of quasi-distributed fluorescent chemosensors on optical fibers can be increased by using a second fiber as an optical delay line. Since the fiber−fiber coupling is evanescent, the intensity losses in the fiber core are kept small, making large arrays of sensors feasible. Given the small, effective sample volume, the detection sensitivity is remarkable, with the potential of further improvement.

(29) Yguerabide, J.; Yguerabide, E. E. *Anal. Biochem.* **1998**, *262*, 137−156.
(30) Yguerabide, J.; Yguerabide, E. E. *Anal. Biochem.* **1998**, *262*, 157−176.

ACKNOWLEDGMENT

We thank Professor Brian Armstrong (Department of Electrical Engineering, University of Wisconsin−Milwaukee) for lending us his HP 300-MHz digital oscilloscope used in the early stages of this work. Financial support by the National Science Foundation Grants CHE-0078895 (P.G.) and CHE-9874241 (A.W.S.) is gratefully acknowledged.

Received for review September 25, 2000. Accepted November 27, 2000.

AC0011437